

Optimizing photoelectrochemical properties of TiO₂ by chemical codoping

Peng Wang,¹ Zhirong Liu,² Feng Lin,¹ Gang Zhou,¹ Jian Wu,¹ Wenhui Duan,^{1,*} Bing-Lin Gu,¹ and S. B. Zhang^{3,†}

¹Department of Physics, Tsinghua University, Beijing 100084, People's Republic of China

²College of Chemistry and Molecular Engineering, Peking University, Beijing 100871, People's Republic of China

³Department of Physics, Applied Physics, and Astronomy, Rensselaer Polytechnic Institute, Troy, New York 12180, USA

(Received 16 September 2010; published 23 November 2010)

First-principles calculations reveal potentially optimal photoelectrochemical activity of anatase TiO₂ by means of (C, S), (C, Se), or (N, P) codoping. It is found that the absorption edge is substantially redshifted to visible regime with overall spectra considerably better than monodoped TiO₂. The resulting optical gap straddle the redox potentials of H₂O remarkably well. The reason for the significant improvements is the direct chemical bonding between the codopants. We expect this generic band-structure tailoring scheme also applies to other photocatalytic systems and beyond.

DOI: 10.1103/PhysRevB.82.193103

PACS number(s): 71.20.Nr, 61.72.Bb, 71.55.Ht

For its strong photocatalytic activity, high chemical stability, and nontoxicity, TiO₂ has been one of the most promising photocatalysts, for example, for hydrogen production through photoelectrochemical (PEC) water splitting, dye-sensitized solar cell, degeneration of pollutants, and conversion of inorganic molecules to fuels from sunlight.^{1–5} However, applications of TiO₂ are severely limited by its too large (3.2 eV) band gap: pure TiO₂ only absorbs ultraviolet light, which amounts to only ~5% of the total solar-energy spectrum. Band-structure engineering to reduce the gap is therefore highly desirable. Various types of doping, especially *p*-type doping, have been widely used to achieve such a goal.^{6–12} However, monodoping suffers from higher carrier recombination rate because it creates undesirable acceptor (or donor) gap states that reduce the PEC efficiency.^{13,14} One may contain this negative effect of monodoping, for example, by a *p-n* codoping.^{15–18} A more stringent requirement, though, is that any modification of the band gap should simultaneously match the TiO₂ band structure with the redox potentials of water for the best energetics. Because the conduction-band minimum (CBM) of TiO₂ lies slightly above the hydrogen production level while the valence-band maximum (VBM) lies considerably below the water oxidation level, an ideal solution would be to shift only the VBM, not the CBM, while lowering the optical gap. This remaining hurdle prevents the broad deployment of engineered TiO₂ for water splitting.

In this work, we propose a band-structure tailoring scheme via a degenerate codoping or dilute alloying mechanism, which not only narrows the band gap, thereby shifting the absorption edge to the desired visible region, but also in such a way that the narrowed band gap straddles almost perfectly over the redox potentials of water. This is made possible by a special choice of the codopant pairs: e.g., (C, S), (C, Se), or (N, P), both of which occupy only the oxygen sites. As such, the predominant effect of the doping is on the valance band instead of on the conduction band. Qualitatively different from the monodoping by either carbon (which introduces an undesirable empty gap state) or sulfur (which has very little effect on the TiO₂ band gap), the formation of the C-S, C-Se, and N-P second-nearest-neighbor pairs eliminates the empty gap states by forming an extra

bond per pair. Our scheme thus overcomes the difficulties of some previous schemes.

Our calculations were performed primarily using the density-functional theory within the generalized gradient approximation (GGA) by Perdew and Wang (PW91).¹⁹ Projector augmented wave potentials²⁰ were used with a cutoff energy of 520 eV for the plane-wave basis set and a 6 × 6 × 6 Monkhorst-Pack²¹ *k*-point mesh for the Brillouin-zone integration. Our calculated lattice parameters for primitive anatase TiO₂ unit cell are $a=b=3.819$ Å and $c=9.695$ Å, respectively, in good agreement with experiment.²² We used a 2 × 2 × 1 supercell containing 48 atoms, where two O atoms are substituted by the codopants. Structural optimizations were carried out until forces on the atoms are less than 10 meV/Å. GGA severely underestimates the TiO₂ band gap. To ensure reasonably accurate band gaps and band alignments, we performed Heyd-Scuseria-Ernzerhof (HSE) calculations.²³ It yields a TiO₂ band gap of 3.2 eV in good agreement with experiment. All calculations use the Vienna *ab initio* simulation package (VASP).²⁴

A key index to the performance of the modified TiO₂ is its optical absorption, reflected in the imaginary part of the dielectric function, ϵ_2 . Figure 1 depicts ϵ_2 as a function of wavelength and energy for pure, C-, S-, (C, S)-, (C, Se)-, and (N, P)-doped TiO₂. The calculated ϵ_2 for pure TiO₂ agrees with experiment.²⁵ Two distinct features are observed. First, the absorption edges for (C, S)-, (C, Se)-, and (N, P)-doped TiO₂ are much lower than that of pure TiO₂ by 1.60 eV, 1.64 eV, and 2.08 eV, respectively. Second, absorption in the entire visible region is substantial, most noticeably for (N, P) TiO₂ with a peak value, $\epsilon_2 \sim 5$, near its absorption edge and a minimum value, $\epsilon_2 \sim 1.3$, near the absorption edge of TiO₂. The codoped TiO₂'s are thus ideal for absorbing visible light.

To understand the significant improvement, we plot in Fig. 2 the calculated band structures. For C-doped TiO₂ [Fig. 2(a)], three carbon bands (two occupied and one empty) emerge in the original band gap of pure TiO₂. The empty band gives rise to the large redshift in the absorption edge in Fig. 1. It also acts as a recombination center to reduce the PEC efficiency.^{11,15,26} For S-doped TiO₂ (Ref. 11) [Fig. 2(b)], because S is isovalent to O, there exists no empty impurity state inside the band gap except for an upshift of the topmost valence band toward the conduction band. For (C, S)-doped

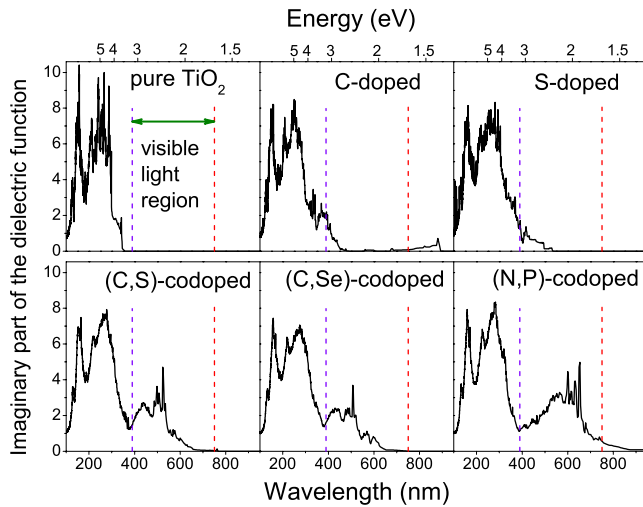


FIG. 1. (Color online) Calculated imaginary part of the dielectric function (ϵ_2) for pure and doped TiO_2 , where the spectrum is shifted according to HSE calculations (i.e., the scissor operator is used). Vertical dashed lines mark the visible light region.

TiO_2 [Fig. 2(c)], the gap states are not simply a combination of those of C- and S-doped TiO_2 , as one might expect from the usual p - n codoped systems.¹⁵ We see, instead, that while the two occupied carbon bands remain, the third, empty carbon band vanishes completely from the gap. The upshift of the TiO_2 valence band due to S doping also disappears.

The calculated projected density of states (PDOS) for the (C, S)-doped TiO_2 in Fig. 2(d) reveals that the CBM states exhibit mainly the Ti $3d$ character and are hardly changed from that of pure TiO_2 . Thus, the modification of the (C, S)-doped TiO_2 band gap comes mainly from the VBM,

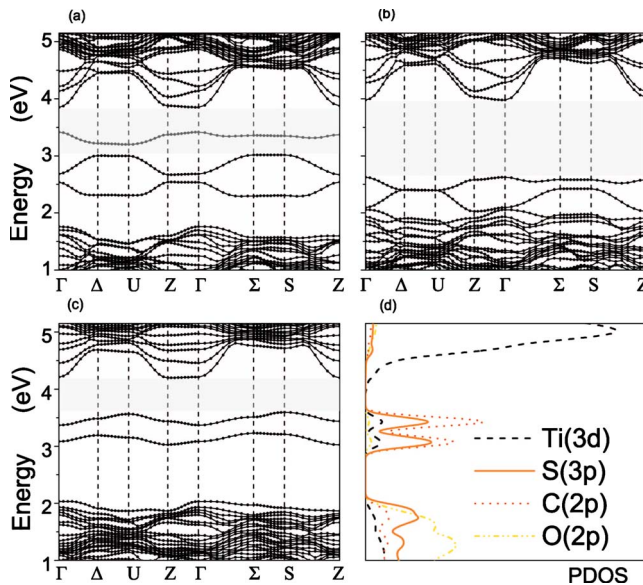


FIG. 2. (Color online) Band structures of (a) C-, (b) S-, and (c) (C, S)-doped TiO_2 . The effective gaps for the absorption are shaded. In panel (a), the unoccupied impurity state is localized and makes little contribution to the absorption, so it is excluded in determining the effective gap. (d) Projected density of states per atom for (C, S)-doped TiO_2 .

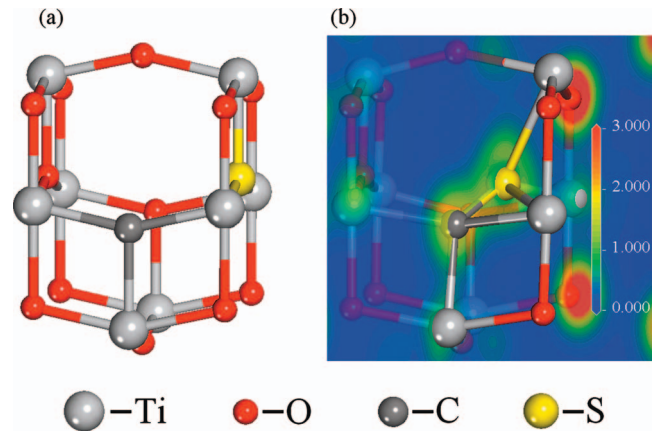


FIG. 3. (Color) Atomic structures of (C, S)-doped TiO_2 (a) before and (b) after atomic relaxation. The total-charge density in (b) in the plane containing both C and S atoms shows clearly the formation of the C-S bond.

which consists of occupied states with C $2p$ and S $3p$ atomic characteristics.

As discussed above, the key observation underlying the exceptional properties of the (C, S)-doped TiO_2 is the removal of the empty carbon band from the band gap. To understand its microscopic origin, we examine the atomic structure of the (C, S) pair, where both C and S occupy the O sites, namely, C_O - S_O . Figure 3 shows that after relaxation, the C and S atoms move toward each other to form a new bond with a bond length $d=1.694$ Å.²⁷ This bond length can be compared to the sum of the atomic radii: $0.77(\text{C})+1.02(\text{S})=1.79$ Å for a strong single chemical bond between C and S and the usual O-O separation in pure TiO_2 of 3.086 Å.

From a chemistry point of view, in C-doped TiO_2 , although the C atom is threefold coordinated, it still has an empty, out-of-plane $2p$ orbital, which appears in Fig. 2(a) as the empty carbon band in the upper half of the band gap. In S-doped TiO_2 , on the other hand, the S atom is also threefold coordinated with a doubly occupied $3p$ orbital sticking out of its own bonding plane. This lone-pairlike orbital contributes to the upshift of the VBM of S-doped TiO_2 in Fig. 2(b). There is thus a natural tendency for the C and S to bind together through a mixing of their out-of-plane orbitals. The net result is a significant lowering of the C-S bonding state deep into the valence band and a significant rising of the C-S antibonding state deep into the conduction band.

Consequently, the C-derived empty band vanishes from the band gap. As a secondary effect, the two C-derived occupied gap states in Fig. 2(a) hybrid with the S-derived top-most occupied states in Fig. 2(b) to clear the latter completely from the band gap. This leaves behind with only the two C-derived occupied states of mixed atomic C and S characters with energies somewhat higher than those of the C monodoped TiO_2 in Fig. 2(a). In theory, the binding mechanism discussed here should also work for a (C, O) pair. However, the atomic radius of O is only 0.73 Å. The formation of a C-O bond would give rise to a too large strain that is energetically disfavored. Thus, the codoping principle, characterized by the formation of a chemical bond between the

TABLE I. Binding energy (E_B) and formation energy (ΔH) for different (C, S) pairs (in units of electron volt), where C_O and C_{Ti} stand for substitutional C for O and Ti, respectively, and C_i stands for interstitial C. This convention also holds for S.

	C_O-S_O	C_i-S_O	C_O-S_i	$C_{Ti}-S_i$	C_i-S_{Ti}	$C_{Ti}-S_O$
E_B	3.21	0.04	4.38	1.13	1.79	-0.70
ΔH (O-poor)	0.27	3.68	3.71	10.36	10.75	7.65
ΔH (O-rich)	9.72	8.41	8.44	0.90	1.28	2.92

codopants, emerges for the design of future PEC materials. It has two basic elements: (a) the codopants should have a net less number of electrons than the two host O atoms by two and (b) the size of the codopant atoms should be larger than that of O. Following this principle, we have designed the (C, Se) and (N, P) pairs. Indeed, they both showed the desired properties (see Fig. 1). Note that N and P, substituting for oxygen, are both electronic single acceptors, which in the conventional codoping picture can only entail Coulomb repulsion between them.

The formation of the strong chemical bond lowers the energy of the pair considerably, for example, by 3.32 eV for the (C, S) pair. This energy lowering, however, diminishes if the C and S are fourth- or sixth-nearest neighbors, which establishes the origin of the codoping to be chemical, not electrical. One may calculate the formation energy of the pair, defined as²⁸

$$\Delta H = E_{\text{tot}}(\text{C,S}) - E_{\text{tot}}(\text{pure}) - \mu_C - \mu_S + 2\mu_O,$$

where $E_{\text{tot}}(\text{C,S})$ and $E_{\text{tot}}(\text{pure})$ are the total energy of (C, S)-doped and pure TiO_2 , μ_C , μ_S , and μ_O are the chemical potentials of C, S, and O, respectively. Most likely the growth of an engineered TiO_2 will not be an equilibrium process but a kinetic process. Hence, we will use a kinetic solubility theory, which has previously been applied to N-doped ZnO,²⁹ N-doped GaAs,³⁰ and B-doped Si.³¹ In such an theory, we consider the existing but not necessarily the most stable form of the dopants, e.g., bulk diamond and S_2 gas, to obtain ΔH .

For simplicity, our discussion so far assumes single (C, S) configuration, namely, C_O-S_O . If we consider also substitution for Ti and interstitials, there would be $3 \times 3 = 9$ different combinations for the (C, S) pairs. Table I lists ΔH for six lowest-energy configurations: three at the O-poor and three at the O-rich conditions. The C_O-S_O pair is among those with strongest binding energies. It also has the lowest $\Delta H = 0.27$ eV under the O-poor condition. We also calculated the formation energy of a C_O-C_O pair to be 0.99 eV. This value is nearly four times that of a (C, S) pair, suggesting that aggregation of substitutional carbon is unlikely.

Next, we address the most critical issue, namely, the energetics of the chemically codoped TiO_2 , for PEC water splitting. To do so, we need to determine the relative VBM positions between pure and the various doped TiO_2 to align them all on one diagram. This was done by using the $3s$ core levels of the Ti atoms farthest away from the dopants. Our calculated variance in the alignment is less than 0.05 eV, which justifies the use of such an approach. The relative

positions between the H_2O redox potentials and the band edges of pure TiO_2 are, on the other hand, obtained from experiment.³

Figure 4 summarizes the results. Note that here the energy is relative to the normal hydrogen electrode (NHE), and the energy increases as the electron energy (in the standard energy diagram) decreases. Pure TiO_2 , our reference system, has the VBM farthest away from the water oxidation level ($\text{H}_2\text{O}/\text{O}_2$).³ Monodoping or (Mo, C) codoping, which represents one of the best scenarios for the p - n codoping scheme, reduce this energy offset, but the chemical codoping has unique advantages with its VBM only a few tenths of an electron volt away from the $\text{H}_2\text{O}/\text{O}_2$ level. For the hydrogen production level ($\text{H}_2/\text{H}_2\text{O}$), the chemically codoped TiO_2 show practically no difference and all the calculated CBMs are similar to that of pure TiO_2 as desired. This is understood because all the dopants here are on the anion sites. The gap of (N, P)-codoped TiO_2 (1.1 eV) is noticeably smaller than the desired gap (1.6–2.2 eV), indicating a lower PEC efficiency in comparison with (C, S)-codoped system.

In summary, PEC water splitting for hydrogen production faces the daunting challenge to meet not one but three requirements: (1) stability, (2) efficiency (namely, the band gap should be between 1.6 and 2.2 eV), and (3) energetics (namely, the band edges should straddle the H_2O redox potential levels), must be simultaneously satisfied.³² Pure TiO_2 is qualified only for its stability. Electrical codoping can also

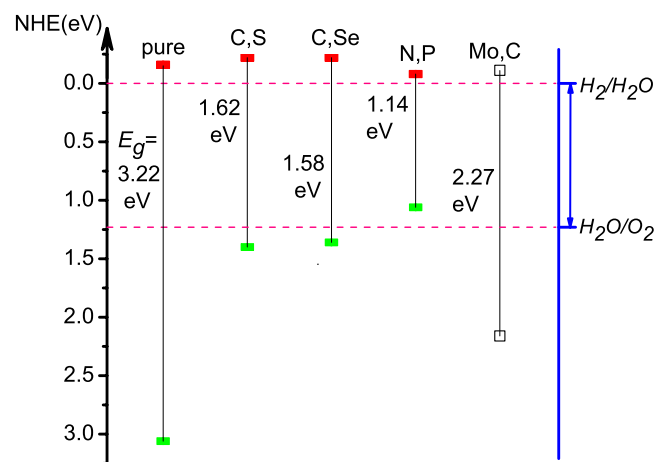


FIG. 4. (Color online) Conduction-band minimum (red/gray) and valence-band maximum (green/light gray) relative to the NHE for pure and various doped TiO_2 . The value for (Mo, C)-codoped TiO_2 (which is representative of optimal p - n codoping) is taken from Ref. 15 for comparison.

improve the efficiency but not the energetics. By comparison, the chemical codoping principle proposed here has the potential to meet all three requirements. Because the basic principle for gap engineering is completely general, we expect the chemical codoping to work beyond the design of photochemical catalysts.

This work was supported by the Ministry of Science and Technology of China (Grants No. 2006CB605105 and No. 2006CB0L0601) and the National Natural Science Foundation of China. S.B.Z. was supported by the U.S. Department of Energy under Grant No. DE-SC0002623 and the DOE/BES/CMSN program.

*dwh@phys.tsinghua.edu.cn

†zhangs9@rpi.edu

- ¹A. Fujishima and K. Honda, *Nature (London)* **238**, 37 (1972).
- ²M. R. Hoffmann, S. T. Martin, W. Y. Choi, and D. W. Bahnmann, *Chem. Rev.* **95**, 69 (1995).
- ³M. Grätzel, *Nature (London)* **414**, 338 (2001).
- ⁴S. U. M. Khan, M. Al-Shahry, and W. B. Ingler, Jr., *Science* **297**, 2243 (2002).
- ⁵G. K. Mor, K. Shankar, M. Paulose, O. K. Varghese, and C. A. Grimes, *Nano Lett.* **6**, 215 (2006); O. K. Varghese, M. Paulose, T. J. LaTempa, and C. A. Grimes, *ibid.* **9**, 731 (2009).
- ⁶R. Asahi, T. Morikawa, T. Ohwaki, K. Aoki, and Y. Taga, *Science* **293**, 269 (2001).
- ⁷M. Batzill, E. H. Morales, and U. Diebold, *Phys. Rev. Lett.* **96**, 026103 (2006).
- ⁸C. Di Valentin, G. Pacchioni, and A. Selloni, *Phys. Rev. B* **70**, 085116 (2004); *Chem. Mater.* **17**, 6656 (2005); N. Serpone, *J. Phys. Chem. B* **110**, 24287 (2006).
- ⁹T. Ohsawa, I. Lyubinetsky, Y. Du, M. A. Henderson, V. Shutthanandan, and S. A. Chambers, *Phys. Rev. B* **79**, 085401 (2009); E. Mete, D. Uner, O. Gülseren, and Ş. Ellialtıoğlu, *ibid.* **79**, 125418 (2009); J. Y. Lee, J. Park, and J. H. Cho, *Appl. Phys. Lett.* **87**, 011904 (2005).
- ¹⁰F. M. Hossain, L. Sheppard, J. Nowotny, and G. E. Murch, *J. Phys. Chem. Solids* **69**, 1820 (2008).
- ¹¹T. Umebayashi, T. Yamaki, H. Itoh, and K. Asai, *Appl. Phys. Lett.* **81**, 454 (2002); *J. Phys. Chem. Solids* **63**, 1909 (2002).
- ¹²R. Nakamura, T. Tanaka, and Y. Nakato, *J. Phys. Chem. B* **108**, 10617 (2004); T. Ohno, M. Akiyoshi, T. Umebayashi, K. Asai, T. Mitsui, and M. Matsumura, *Appl. Catal., A* **265**, 115 (2004).
- ¹³D. C. Cronemeyer, *Phys. Rev.* **113**, 1222 (1959).
- ¹⁴W. Y. Choi, A. Termin, and M. R. Hoffmann, *J. Phys. Chem.* **98**, 13669 (1994).
- ¹⁵Y. Gai, J. Li, S. S. Li, J. B. Xia, and S.-H. Wei, *Phys. Rev. Lett.* **102**, 036402 (2009).
- ¹⁶D. Li, H. Haneda, S. Hishita, and N. Ohashi, *Chem. Mater.* **17**, 2596 (2005).
- ¹⁷W. Zhu, X. Qiu, V. Iancu, X.-Q. Chen, H. Pan, W. Wang, N. M. Dimitrijevic, T. Rajh, H. M. Meyer III, M. P. Paranthaman, G. M. Stocks, H. H. Weitering, B. Gu, G. Eres, and Z. Zhang, *Phys. Rev. Lett.* **103**, 226401 (2009).
- ¹⁸W.-J. Yin, H. Tang, S.-H. Wei, M. M. Al-Jassim, J. Turner, and Y. Yan, *Phys. Rev. B* **82**, 045106 (2010).
- ¹⁹J. P. Perdew and Y. Wang, *Phys. Rev. B* **45**, 13244 (1992).
- ²⁰G. Kresse and D. Joubert, *Phys. Rev. B* **59**, 1758 (1999).
- ²¹H. J. Monkhorst and J. D. Pack, *Phys. Rev. B* **13**, 5188 (1976).
- ²²C. J. Howard, T. M. Sabine, and F. Dickson, *Acta Crystallogr., Sect. B: Struct. Sci.* **47**, 462 (1991).
- ²³J. Heyd, G. E. Scuseria, and M. Ernzerhof, *J. Chem. Phys.* **118**, 8207 (2003); J. Heyd and G. E. Scuseria, *ibid.* **120**, 7274 (2004).
- ²⁴G. Kresse and J. Furthmüller, *Phys. Rev. B* **54**, 11169 (1996).
- ²⁵N. Hosaka, T. Sekiya, C. Satoko, and S. Kurita, *J. Phys. Soc. Jpn.* **66**, 877 (1997).
- ²⁶W. Mu, J. M. Herrmann, and P. Pichat, *Catal. Lett.* **3**, 73 (1989).
- ²⁷Larger supercell calculations with 96 and 192 atoms (including one C and one S) have been performed. The results show that the (C, S) pair forms regardless the cell size.
- ²⁸S. B. Zhang and J. E. Northrup, *Phys. Rev. Lett.* **67**, 2339 (1991).
- ²⁹Y. Yan, S. B. Zhang, and S. T. Pantelides, *Phys. Rev. Lett.* **86**, 5723 (2001).
- ³⁰S. B. Zhang and S.-H. Wei, *Phys. Rev. Lett.* **86**, 1789 (2001).
- ³¹X. Luo, S. B. Zhang, and S.-H. Wei, *Phys. Rev. Lett.* **90**, 026103 (2003).
- ³²J. A. Turner, Proceedings of the International Workshop on Direct Photoelectrochemical Production of Hydrogen, Solar-Hydrogen, Adelphi, Maryland, November 9, 2004 (unpublished).